AFRL-RX-WP-TP-2011-4399

CHARACTERIZING RANDOMLY ANISOTROPIC SURFACES IN EDDY-CURRENT NDE (PREPRINT)

Harold A. Sabbagh, R. Kim Murphy, and Elias H. Sabbagh

Victor Technologies, LLC

John C. Aldrin

Computational Tools

DECEMBER 2011

Approved for public release; distribution unlimited.

See additional restrictions described on inside pages

STINFO COPY

AIR FORCE RESEARCH LABORATORY
MATERIALS AND MANUFACTURING DIRECTORATE
WRIGHT-PATTERSON AIR FORCE BASE, OH 45433-7750
AIR FORCE MATERIEL COMMAND
UNITED STATES AIR FORCE

REPORT DOCUMENTATION PAGE	*Form Approved* *OMB No. 0704-0188*

1. REPORT DATE *(DD-MM-YY)*	2. REPORT TYPE	3. DATES COVERED *(From - To)*
December 2011	Journal Article Preprint	01 March 2011 – 01 March 2011

4. TITLE AND SUBTITLE
CHARACTERIZING RANDOMLY ANISOTROPIC SURFACES IN EDDY-CURRENT NDE (PREPRINT)

5a. CONTRACT NUMBER FA8650-09-C-5232

5b. GRANT NUMBER

5c. PROGRAM ELEMENT NUMBER 65502F

6. AUTHOR(S)
Harold A. Sabbagh, R. Kim Murphy, and Elias H. Sabbagh (Victor Technologies, LLC)
John C. Aldrin (Computational Tools)

5d. PROJECT NUMBER 3005

5e. TASK NUMBER ML

5f. WORK UNIT NUMBER LP106T02

7. PERFORMING ORGANIZATION NAME(S) AND ADDRESS(ES)
Victor Technologies, LLC
2609 S. Spicewood Lane
Bloomington, IN 47401

Computational Tools
Gurnee, IL

8. PERFORMING ORGANIZATION REPORT NUMBER

9. SPONSORING/MONITORING AGENCY NAME(S) AND ADDRESS(ES)
Air Force Research Laboratory
Materials and Manufacturing Directorate
Wright-Patterson Air Force Base, OH 45433-7750
Air Force Materiel Command
United States Air Force

10. SPONSORING/MONITORING AGENCY ACRONYM(S) AFRL/RXLP

11. SPONSORING/MONITORING AGENCY REPORT NUMBER(S) AFRL-RX-WP-TP-2011-4399

12. DISTRIBUTION/AVAILABILITY STATEMENT
Approved for public release; distribution unlimited.

13. SUPPLEMENTARY NOTES
PAO Case Number: 88ABW 2011-4534; Clearance Date: 19 Aug 2011. Document contains color.
Journal article submitted to *Review of Progress in QNDE*.

14. ABSTRACT
This research is motivated by two distinct considerations: the ability to model noise in Ti-6Al-4V, and to characterize surfaces that have undergone treatment due to shot-peening, low-plasticity burnishing, etc. We will show that with a single model we can analyze these sources of noise and develop a protocol and system requirements for detecting and inverting flaws in a random background. An important result of this study is the application of simple statistical theory toward the development of estimation-theoretic metrics.

15. SUBJECT TERMS
eddy-current nondestructive evaluation, random anisotropic media, electromagnetic inverse problems, estimation-theoretic metrics

16. SECURITY CLASSIFICATION OF: a. REPORT	b. ABSTRACT	c. THIS PAGE	17. LIMITATION OF ABSTRACT:	18. NUMBER OF PAGES	19a. NAME OF RESPONSIBLE PERSON (Monitor)
Unclassified	Unclassified	Unclassified	SAR	14	Jason Heebl
					19b. TELEPHONE NUMBER *(Include Area Code)* N/A

Standard Form 298 (Rev. 8-98)
Prescribed by ANSI Std. Z39-18

CHARACTERIZING RANDOMLY ANISOTROPIC SURFACES IN EDDY-CURRENT NDE

Harold A. Sabbagh[1], John C. Aldrin[2], R. Kim Murphy[1] and Elias H. Sabbagh[1]

[1] Victor Technologies, LLC, Bloomington, IN
[2] Computational Tools, Gurnee, IL

ABSTRACT. This research is motivated by two distinct considerations: the ability to model noise in Ti-6Al-4V, and to characterize surfaces that have undergone treatment due to shot-peening, low-plasticity burnishing, etc. We will show that with a single model we can analyze these sources of noise and develop a protocol and system requirements for detecting and inverting flaws in a random background. An important result of this study is the application of simple statistical theory toward the development of estimation-theoretic metrics.

Keywords: Eddy-Current Nondestructive Evaluation, Random Anisotropic Media, Electromagnetic Inverse Problems, Estimation-Theoretic Metrics
PACS: 02.50.-r, 81.70.-q

STATEMENT OF THE PROBLEM

Ti-6Al-4V is known to be 'noisy,' and this leads to problems in predicting the detectability of small flaws in this alloy. We have already alluded to the fact that because Ti64 has a hexagonal crystal structure, one source of noise would be a random distribution of crystallite orientations, which would result in spatial variations in the local host conductivity. There are other sources such as liftoff and surface 'noise' due to a rough surface profile [1], [2]. We are interested in answering the questions: Can we distinguish noise due to (1) random grids, (2) liftoff, and (3) surface conditions? Can we include these sources in one model of a randomly anisotropic surface?

THE VIC-3D© MODELS

Figure 1 illustrates two models that will start the discussion. The top portion illustrates a simple random, isotropic grid that will be used to estimate the noise due to random spatial inhomogenieties of conductivity, whereas the bottom portion models a simple random patch that simulates surface roughness. This patch is distinguished by randomly interspersing grid elements whose conductivity is zero (representing air) with those whose conductivity is identical to the host's. The height of the surface roughness patch is typical of surface roughness effects as studied in [1]. Neither of these models includes a non-random flaw.

We ran ten samples of each random model on a $32 \times 32 \times 2$ grid, at a frequency of 2MHz, using an air-core coil whose inner radius is 0.555mm, outer radius is 0.855mm,

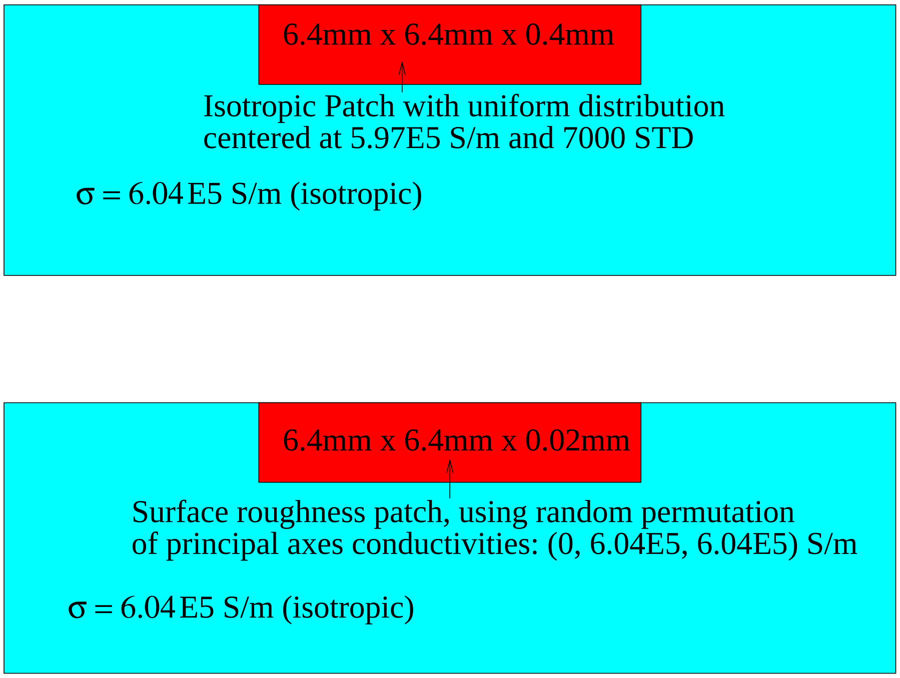

FIGURE 1. Illustrating the **VIC-3D©** models for a random patch (top) and surface roughness (bottom) with no included flaws. Each grid comprises $32 \times 32 \times 2$ cells.

height of 1.12mm, containing 49 turns, and the results are shown in Figure 2. It is clear that for these parameters the surface-roughness model produces a significantly larger response than the random-patch model, which is plausible, given the much greater contrast in conductivities in the surface-roughness model than in the random-patch model. The statistics for this ensemble are shown in Figure 3.

AN INVERSE PROBLEM

In order to determine an equivalent non-random conductivity for the 'Surface roughness patch' shown in the bottom of Figure 1, we will solve an inverse problem for the two principal-axis conductivities, σ_1, σ_2, and depth, H, using the ensemble averages shown in the bottom of Figure 3 as inputs to NLSE. σ_3 is fixed at 4×10^5S/m. The results are shown in Table 1. The results comparing the input data with the computed model data that use the parameters listed in Table 1 are shown in Figure 4.

INVERSE PROBLEM NO. 2: NOISE AND DETERMINISTIC FLAWS

Now we consider a composite problem of a half-penny crack inserted into the rough surface patch shown at the bottom of Figure 1. The crack is modeled as a clipped elliptic cylinder that has been rotated ninety degrees. The semi-axes of the

TABLE 1. Results for inverse problem with $\sigma_{1,2}$ and H unknown.

Φ	σ_1/sensit	σ_2/sensit	H/sensit	No. points
0.2001(-2)	4.00×10^5/3.109(-2)	5.11×10^5/3.039(-2)	0.0186/2.035(-2)	470

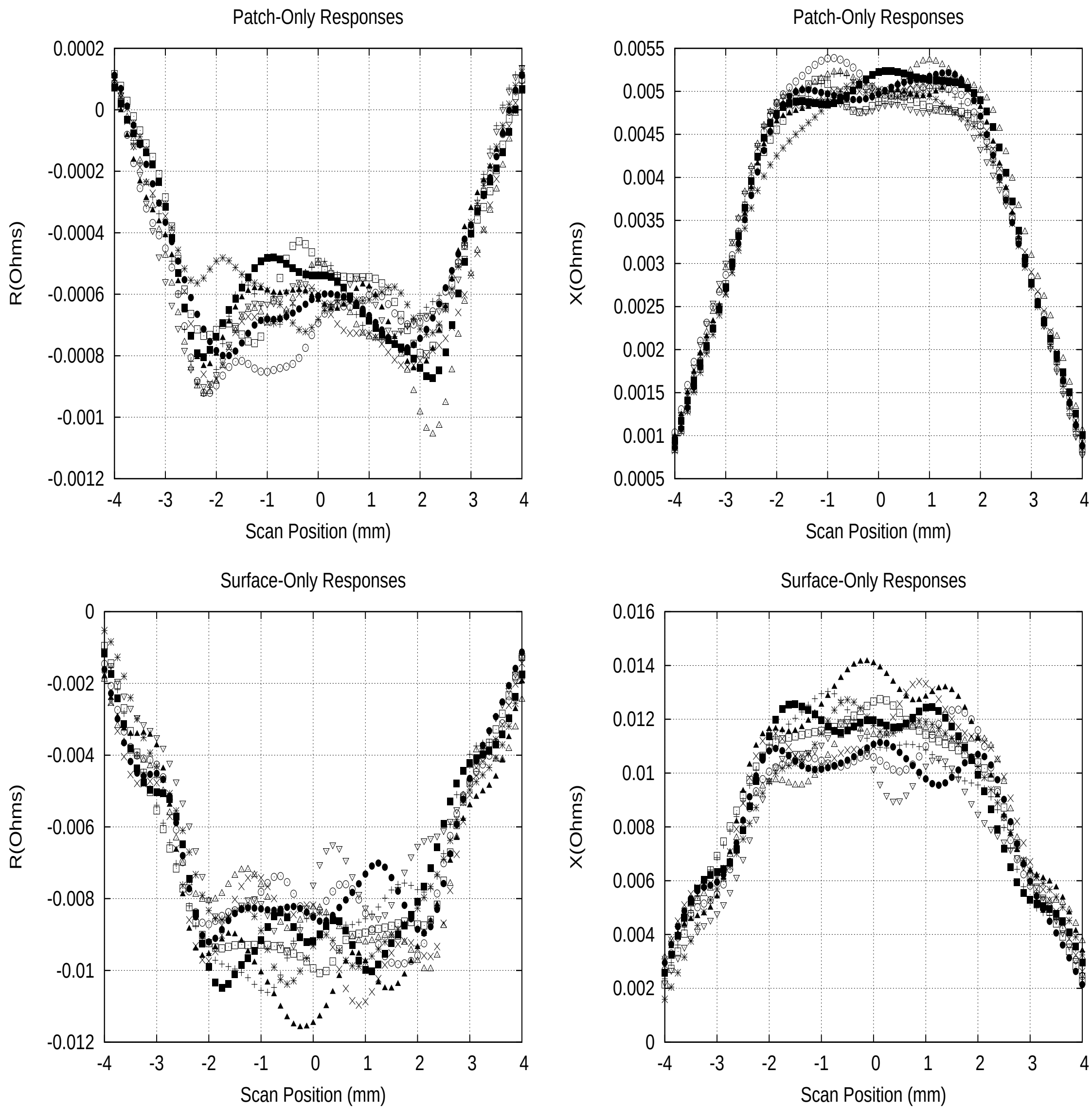

FIGURE 2.10 sample functions for the same model problems shown in Figure 1. Top: Patch only. Bottom: Surface only.

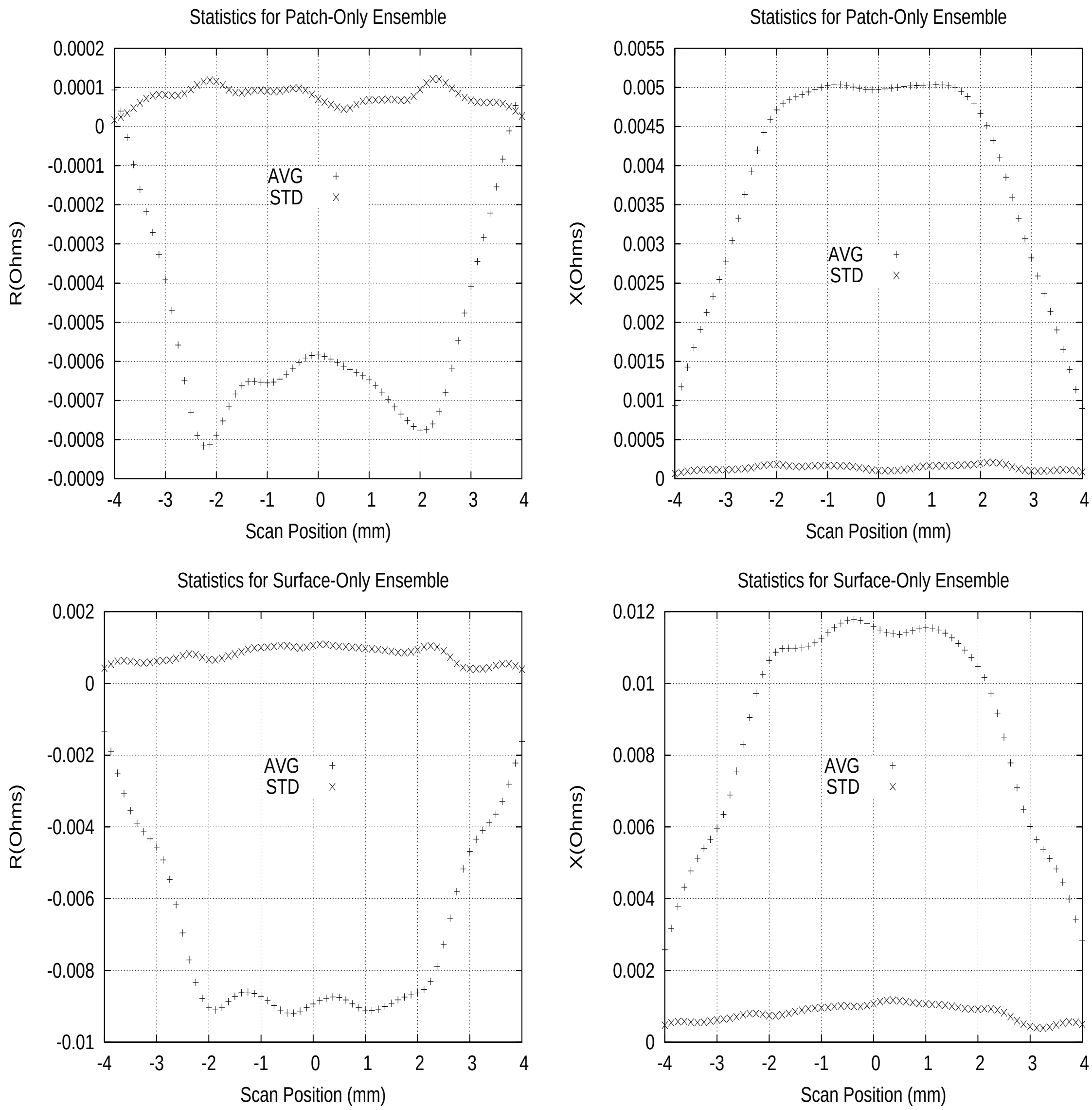

FIGURE 3. Ensemble average and standard deviation of the 10 sample functions shown in Figure 2. Top: Patch only. Bottom: Surface only.

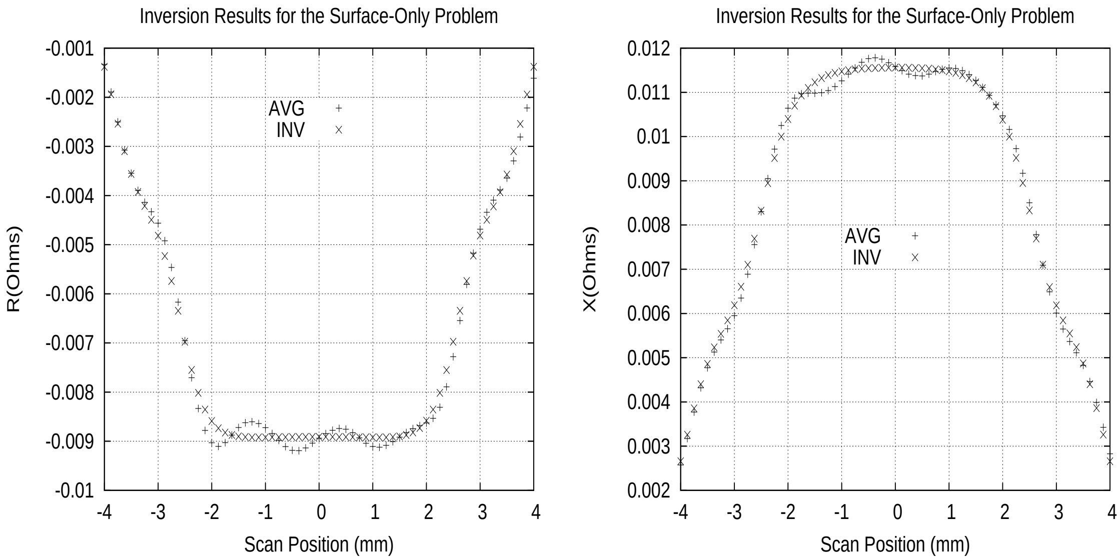

FIGURE 4. Comparing the input data (AVG) for the first inverse problem with the computed model data (INV) that use the parameters listed in Table 1.

cylinder are $A = 0.1693$ mm (depth), and $B = 0.254$ mm (length), and the opening of the crack is 0.1mm. The input sample functions are generated using the random permutation algorithm, but in the interpolation table the random surface patch is replaced with a nonrandom, homogeneous patch with conductivities of $\sigma_1 = 4.0024 \times 10^5$ S/m, $\sigma_2 = 5.1091 \times 10^5$ S/m, $\sigma_3 = 4 \times 10^5$ S/m, and whose depth is 0.0186 mm. These are the parameters shown in Table 1. The unknowns are A, B, and liftoff, LO. The results of a Monte Carlo run with thirty samples are shown in Table 2.

ESTIMATION-THEORETIC METRICS

We can use the results of the Monte Carlo study shown in Table 2 to generate some *a posteriori* metrics, i.e., metrics that follow from the inversion results, which, of course, follow from the measured data. This is in contrast with*a priori* metrics, which precede acting upon measurements. Our goal is to eventually generate the concept of an *a posteriori* 'probability of inversion,' as opposed to the concept of an *a priori* 'probability of detection.'

Table 3 displays the convergence of the various metrics as a function of the number of samples. In this table, $A^* = A - 0.1693$, $B^* = B - 0.254$, S_A denotes the sensitivity of the A estimate, and S_B denotes the sensitivity of the B estimate.

Note that Φ_{STD} is comparable in value to the curves marked 'STD' in the bottom part of Figure 3, so it is reasonable to infer that Φ_{STD} is due to the stochastic process that is producing the noise in the first place. It appears that the estimates for A^*_{avg} and B^*_{avg} are converging, but it's not clear that they are converging to zero, as we would expect from their definitions. In any case, A^*_{avg} is converging to its limit from above, whereas B^*_{avg} is converging from below. If the true limit is zero for each variable, then it is clear that A^*_{avg} is converging more rapidly than B^*_{avg}. This appears to be consistent with the relative values of the standard deviations, A^*_{STD} and B^*_{STD}, of the two variables, with the latter being almost twice the former. The fact that A^*_{avg} and B^*_{avg} may not be converging to zero suggests that this is a 'biased estimator' in the statistical sense,

TABLE 2. Results of Inverse Problem No. 2 With LO Variable.

Sample	Φ	A/sensit	B/sensit	LO/sensit	No. Pts
1	0.6388(-2)	0.2317/0.5525	0.1487/0.1760	5.4(-4)/0.3769	494
2	0.5486(-2)	0.1774/0.2736	0.2088/0.2098	1.032(-2)/0.3130	500
3	0.5692(-2)	0.1746/0.2318	0.2461/0.2333	2.304(-2)/0.3124	500
4	0.5905(-2)	0.1545/0.1785	0.3000/0.2736	2.0(-2)/0.3162	500
5	0.6679(-2)	0.1790/0.3049	0.2151/0.2428	1.438(-9)/0.2305	270
6	0.7960(-2)	0.1589/0.2893	0.2554/0.3416	8.90(-3)/0.4386	499
7	0.8533(-2)	0.2015/0.4444	0.2059/0.2897	1.528(-2)/0.4780	500
8	0.7155(-2)	0.1619/0.2306	0.2777/0.3013	9.343(-3)/0.3865	494
9	0.5979(-2)	0.2050/0.3473	0.1894/0.1938	8.326(-3)/0.3400	500
10	0.8510(-2)	0.1656/0.3211	0.2433/0.3369	4.403(-10)/8.15(-2)	122
11	0.5034(-2)	0.1502/0.1718	0.2771/0.2429	2.243(-2)/0.2749	498
12	0.7815(-2)	0.171/0.3183	0.2314/0.2988	1.397(-9)/0.299	230
13	0.5065(-2)	0.1808/0.225	0.2205/0.1843	2.982(-3)/0.2831	500
14	0.4762(-2)	0.1492/0.1569	0.300/0.2496	3.9977(-2)/0.2560	444
15	0.6970(-2)	0.1807/0.3279	0.2252/0.2774	2.504(-2)/0.3879	500
16	0.7638(-2)	0.1540/0.2974	0.2383/0.3277	1.7835(-9)/0.3849	230
17	0.5957(-2)	0.2045/0.4218	0.1710/0.1976	1.345(-2)/0.3454	500
18	0.9506(-2)	0.1655/0.3228	0.2775/0.4108	2.168(-2)/0.5120	500
19	0.6228(-2)	0.1521/0.2099	0.2860/0.3058	2.995(-2)/0.3373	499
20	0.5762(-2)	0.1573/0.1821	0.2805/0.2490	7.955(-3)/0.3119	479
21	0.9190(-2)	0.1497/0.2719	0.3000/0.4316	1.508(-2)/0.4939	437
22	0.5859(-2)	0.1562/0.2066	0.2624/0.2585	1.126(-2)/0.3218	493
23	0.5115(-2)	0.1698/0.1997	0.2527/0.2154	2.235(-2)/0.2801	500
24	0.6826(-2)	0.1793/0.3151	0.2173/0.2544	6.829(-3)/0.3829	499
25	0.5654(-2)	0.1914/0.2629	0.2173/0.1977	8.774(-3)/0.3150	498
26	0.7941(-2)	0.1936/0.4339	0.2015/0.2852	1.837(-2)/0.4485	500
27	0.6595(-2)	0.1529/0.2356	0.2601/0.2981	1.134(-2)/0.3637	498
28	0.8179(-2)	0.1464/0.2458	0.3000/0.3997	1.880(-2)/0.4410	420
29	0.9758(-2)	0.1663/0.3730	0.2503/0.4061	1.392(-2)/0.5368	500
30	0.5816(-2)	0.2235/0.4266	0.1627/0.1663	1.537(-8)/0.3304	415

TABLE 3. Convergence of Various Estimation-Theoretic Metrics With Sample Size

No. Samples	10	20	30
Φ_{avg}	0.6892(-2)	0.6651(-2)	0.6799(-2)
Φ_{STD}	0.1096(-2)	0.1286(-2)	0.1381(-2)
A^*_{avg}	0.0117	0.0046	0.0042
A^*_{STD}	2.605(-2)	2.208(-2)	2.253(-2)
A_{STD}			2.214(-2)
$S_{A\text{avg}}$			0.2926
$S_{A\text{STD}}$			9.297(-2)
B^*_{avg}	-0.025	-0.0141	-0.0133
B^*_{STD}	4.898(-2)	4.388(-2)	4.346(-2)
B_{STD}			4.138(-2)
$S_{B\text{avg}}$			0.2752
$S_{B\text{STD}}$			7.114(-2)

TABLE 4. Normalized Sensitivities for A in Table 2

Sample	$S_A \div A$	Sample	$S_A \div A$	Sample	$S_A \div A$
1	2.38	11	1.14	21	1.82
2	1.54	12	1.86	22	1.32
3	1.33	13	1.24	23	1.18
4	1.16	14	1.05	24	1.76
5	1.70	15	1.81	25	1.37
6	1.82	16	1.93	26	2.24
7	2.21	17	2.06	27	1.54
8	1.42	18	1.95	28	1.68
9	1.69	19	1.38	29	2.24
10	1.94	20	1.16	30	1.91

though the amount of the 'bias' is quite small for either A or B.

When we apply this model in practice, we will want to draw a conclusion as to the reliability of the resulting inversion for A and B. (We can't speak in terms of A^* or B^* because in practice we won't know what our target values are.) The only data that we will have that can be used as estimation metrics will be Φ and S_A and S_B. The results in Table 3 will give us typical values of these metrics that we can expect for successful inversions, and if the actual values depart from the averages or STDs that we would expect, then we suspect that we have a bad inversion. Furthermore, $S_{A\text{avg}}$ and $S_{B\text{avg}}$ give us an indication of typical values that we can expect for S_A and S_B, so that we can use this to draw a conclusion as to the reliability of the inverted data in practice.

We have computed the normalized sensitivity parameter for each of the thirty entries in Table 2, and have plotted them in Table 4. There are seventeen that have values below 1.78, and when we average A in Table 2 over these seventeen samples, we get $A_{\text{avg}} = 0.1681$. Clearly, this is a better approximation to the original value of 0.1693 than the value of 0.1735 that was computed in Table 3. The final interesting fact about this result is that when we average B, using the same seventeen samples in Table 2, we obtain $B_{\text{avg}} = 0.2536$, which is impressively close to the original value of 0.254,

all without regard to the normalized sensitivity parameters of B. It appears that the crucial unknown that controls the quality of these inversions is the depth parameter, A, and it appears that the crucial estimation-theoretic metric is the normalized sensitivity parameter associated with A.

We can make contact with classical probability theory by computing the variance of the estimates for the seventeen samples of A in Table 2 for which the normalized sensitivity is below 1.78. A simple calculation shows this to be $\mathrm{VAR}(\widetilde{A}) = 2.655 \times 10^{-4}$, where the tilde denotes the set: $A \ni S_A \div A \leq 1.78$. The Chebychev inequality [3] states that, for any random variable, X, and every $\epsilon > 0$,

$$\mathrm{P}[|X| \geq \epsilon] \leq \frac{1}{\epsilon^2}\mathrm{E}(X^2) \ , \tag{1}$$

which, upon letting $X = \widetilde{A} - 0.1681$, yields

$$\mathrm{P}[|\widetilde{A} - 0.1681| \geq \epsilon] \leq \frac{1}{\epsilon^2} \times 2.644 \times 10^{-4} \ . \tag{2}$$

Suppose that we let $(1/\epsilon^2) \times 2.655 \times 10^{-4} = 0.1$, so that $\epsilon = 5.15 \times 10^{-2}$, then we have the probability estimate $\mathrm{P}[\widetilde{A} \geq 0.2196 \text{ or } \widetilde{A} \leq 0.1166] \leq 0.1$, or

$$\mathrm{P}[0.1166 \leq \widetilde{A} \leq 0.2196] \geq 0.9 \ . \tag{3}$$

Hence, we can say that with at least 90% certainty, those estimates, A, for which $S_A \div A \leq 1.78$ correspond to cracks that have depths lying in the range $[0.1166,\ 0.2196]$.

COMMENTS AND CONCLUSIONS

We applied model-based inversion to replace a randomly inhomogeneous anomaly with a homogeneous, nonrandom anomaly which is to be used in subsequent inverse problems. Because we have modified the actual configuration of an inhomogeneous region with an 'equivalent' homogeneous one, various other parameters will be affected, such as the liftoff of the probe. Hence, we must solve for this parameter, as well as the desired ones that characterize the flaw, in our interpolation table. The fact that we got good statistical results for the inversions suggest that this transformation is a viable way of applying model-based inversion. This approach also led to the recognition of the importance of 'normalized sensitivities' as a metric of reliability of the inversion.

ACKNOWLEDGMENTS

This work was supported by the Air Force Research Laboratory through contract FA8650-09-C-5232 with Victor Technologies LLC.

REFERENCES

1. Yu, F., and Nagy, P. B., "Numerical method for calculating the apparent eddy current conductivity loss on randomly rough surfaces," *J. App. Physics*, **95**, 12, 15 June 2004, pp. 8340-8351.
2. Kalyanasundaram, K., and Nagy, P. B., "A simple numerical model of the apparent loss of eddy current conductivity due to surface roughness," *NDT&E International*, **37**, 2004, pp. 47-56.
3. M. Loève, *Probability Theory*, D. Van Nostrand, New York, 1955.